Phase II Scintigraphic Clinical Trial of Malignant Melanoma and Metastases with Iodine-123-N-(2-Diethylaminoethyl 4-Iodobenzamide)

J.M. Michelot, M.F.C. Moreau, A.J. Veyre, J.F. Bonafous, F.J. Bacin, J.C. Madelmont, F. Bussiere, P.A. Souteyrand, L.P. Mauclaire, F.M. Chossat, J.M. Papon, P.G. Labarre, Ph. Kauffmann and R.J. Plagne

INSERM U 71, Clermont-Ferrand, France; CHU Gabriel Montpied, Clermont-Ferrand, France; Centre Antoine Lacassagne, Nice, France; Hôtel-Dieu, Clermont-Ferrand, France; and CIS biointernational, Gif-Sur-Yvette, France

Preclinical studies established [^{125}I]-N-(2-diethylaminoethyl) 4-iodobenzamide (BZA) as a potential radiopharmaceutical in the management of patients with malignant melanoma. External detection of both murine and human melanotic melanomas was possible after intravenous injection of ^{125}I-BZA in tumor-bearing mice. This article reports a Phase II clinical trial evaluating ^{123}I-BZA as an imaging agent of primary melanomas and metastases. A total of 110 patients with a history of melanoma were investigated in two nuclear medicine departments. Subjects were imaged from 20 to 24 hr after the intravenous injection of 3.5 mCi (130 MBq) of ^{123}I-BZA. After injection, no short-term or long-term side effects were noted. Calculated on a lesion-site basis, diagnostic sensitivity was 81%, accuracy was 87% and specificity was 100%. The melanoma nature of previously occult lesions was confirmed by clinical criteria and/or additional investigations in follow-up studies. The scintigraphies were normal in 44 patients in clinical remission after treatment of malignant melanoma and in seven patients with nonmelanoma disease. No false positive results were observed. Iodine-123-BZA scintigraphy appears to be a safe and useful agent for the detection and follow-up of patients with malignant melanoma. BZA also allowed the detection of unsuspected lesions and the evaluation of the results of various therapeutic procedures such as surgery, chemotherapy, immunobiology, biological therapy or radiotherapy.

J Nucl Med 1993; 34:1260–1266

Despite skin cancer education in the past decade, the incidence of malignant melanoma (MM) has soared dramatically between 1982 and 1989 (*1*). MM is also a neoplasia characterized by an impressive degree of malignancy. This tumor requires a multidisciplinary approach both in diagnosis and therapy (*2*). More specifically, diagnostic accuracy is rendered difficult by the multiplicity of localizations and the difficulty of diagnosis.

Several preclinical studies have identified radiopharmaceuticals as likely agents to localize melanomas in nuclear medicine. Agents with melanine affinity such as quinolines (*3*), melanine precursors such as thiouracil (*4*) and nonspecific tumor localizing agents such as gallium (*5*), have been evaluated and have had limited success. Nuclear medicine has added a new dimension in the localization of tumors in the last decade by means of radiolabeled monoclonal antibodies (Mab) against tumor-associated antigens with both diagnostic and therapeutic purposes (*6*). The largest multicenter clinical trial of radioimmunoscintigraphy (RIS) in melanoma is the study of the Ferrone monoclonal antibody against the high molecular weight melanoma antigen 225-28 S (*7*). Seventy-four percent of lesions were visualized with ^{99m}Tc-F(ab')$_2$. Skin nodules were visualized less frequently and usually the small lesions (<2 cm) were not detected. RIS has also been used in conjunction with conventional investigations in the differential diagnosis of ocular melanomas from other metastases or benign choroidal tumors with a sensitivity of 77% and a specificity of 99% (*8*).

We previously reported preclinical studies showing uptake of N-(2-diethylaminoethyl) 4-iodobenzamide (^{125}I-BZA) in tumor-bearing mice. Scintigraphic images of both murine B16 and human melanotic melanoma confirmed that external detection of melanoma was possible with this new iodinated radiopharmaceutical (*9,10*). Secondary ion mass spectrometry (SIMS) microscopy was used to show the tissue localization of iodinated-BZA. Images obtained by an ionic microscope were correlated with those obtained by a light microscope. BZA mapping suggested the localization in the cytoplasm of tumor tissue cells with a

Received Oct. 20, 1992; revision accepted Apr. 5, 1993.
For correspondence or reprints contact: J.M. Michelot, MD, PhD, INSERM U 71, Rue Montalembert, B.P. 184, 63005 Clermont-Ferrand Cedex, France.

heterogeneous distribution correlated to cells containing melanosomes. In C57BL6 mouse eyes, we observed distribution of BZA in the pigmented structures: retina, choroid and ciliary body (Chehade F, *unpublished data*). These preliminary results are indirect proof of the binding of BZA to melanin pigment. These results are still under investigation.

This article reports a Phase II clinical trial evaluating ^{123}I-BZA as an imaging agent of primary malignant melanomas and metastases. This is a bicentric, open, nonrandomized and noncomparative scintigraphic study. This investigation has been approved by the Institutional Ethics Committee of the Clermont-Ferrand School of Medicine.

MATERIAL AND METHODS

Radiopharmaceutical

Because of its simplicity and reliability, the isotopic exchange procedure used for the ^{125}I-labeling of BZA was suitable for the incorporation of ^{123}I (*10*).

Iodine-123-BZA was prepared at CIS biointernational under the following conditions: a solution of 10 mg of BZA in 0.1 *M* citrate buffer with a pH of 4 (0.5 ml) and 1 mg of $CuSO_4$ was added to 260 MBq (7 mCi) of ^{123}I Na (obtained by (p, 5n) reaction). The reaction mixture was heated at 140°C for 40 min. The dry residue was dissolved in 5 ml of 154 mmol NaCl. After passing through a 0.22 μ Millex-GV filter (Millipore, Milford, MA), the solution was ready for intravenous administration.

Radiochemical purity was tested by thin-layer chromatographic (TLC) analysis using Silica gel plates and a mixture of chloroform-aceton-diethylamine (85:12:3) as an eluant. Iodine-123-BZA had a Rf = 0.35; ^{123}I:Rf = 0.05. Radiochemical purity was always ≥98% as controlled by TLC.

Apyrogeneity control was achieved using the Limulus Amebocyte Lysate technique. Sterility controls were achieved using two liquid media (thioglycolate, trypease soja).

Patients

One-hundred and ten patients, (40 male and 70 female, age range 16–89 yr, mean, 60 yr) gave written informed consent and were entered in the study. Scintigraphic examinations were performed in the following manner: (1) an initial check-up (before treatment) for diagnosis of the primary lesions (Group 1, n = 22:1A cutaneous n = 3, 1B ocular n = 19); (2) diagnosis of documented recurrences and metastases after treatment of the primary lesion (lesions were documented by clinical examination, x-ray, computerized tomography (CT), ultrasound investigation, bone scintigraphy and/or biopsy) (Group 2, n = 37); and (3) postmelanoma therapeutic survey of patients in complete clinical remission (Group 3, n = 44).

For some patients, scintigraphy was performed for differential diagnosis when melanoma was only suspected as a possibility among other pathologies (n = 7).

Scintigraphy Protocol

An oral dose (500 mg) of potassium iodide was given to each subject 1 hr before the injection to block the thyroid uptake of the tracer.

A dose of 130 MBq of ^{123}I-BZA in a volume of 5 ml was injected intravenously in 2 min. Tissue distribution was analyzed at different times after injection by analogical and computerized scintigraphy. Scans were taken by standard techniques; anterior and posterior whole-body image (GE, Milwaukee, WI, and Sophy cameras, Sopha Medical, Buc, France) and static views (Gammatome, Sopha Medical). Data were acquired for quantification (S 4000 Sophy, Sopha Medical).

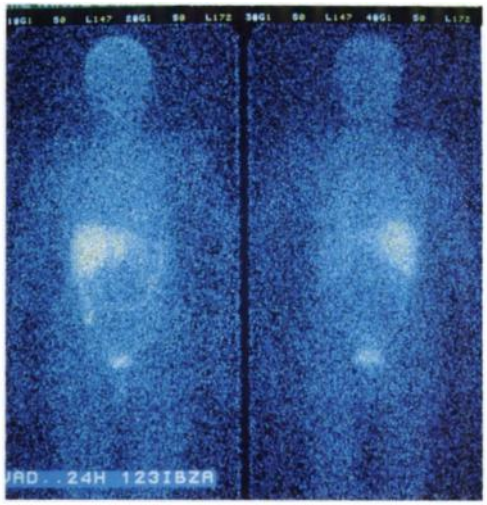

FIGURE 1. Whole-body scan of a Group 3 patient taken 24 hr after intravenous injection of ^{123}I-BZA shows normal uptake in the liver and kidneys (left, anterior; right, posterior).

The imaging data were independently interpreted by two physicians in each nuclear medicine department. Confirmation of occult lesions detected by ^{123}I-BZA scintigraphy was obtained by conventional methods.

Data on pharmacodynamics and pharmacokinetics of the tracer are given in the Appendix.

Statistical Analysis

Statistical analysis of the results of the BZA scintigraphy was performed with the Mac Nemar test comparing scintigraphic imaging with other methodologies of detection of MM. Sensitivity, specificity, accuracy, positive and negative predictive values were calculated on a patient basis and also on a lesion site basis.

RESULTS

After injection of ^{123}I-BZA, no short-term or long-term side effects were observed. The investigators observed normal quickly distributed radioactivity in blood circulation. Qualitative analysis of images shows a number of specific organs which exhibited a significant uptake of ^{123}I-BZA in the early stage of the study; liver, kidneys, brain, salivary glands, lungs and urinary bladder. Six hours postinjection, activity was still high in the liver, kidneys and bladder, and moderate in the lungs and brain. In the normal eye, faint uptake was different from one patient to another but symmetrical. Because of brain activity 6 hr postinjection, eye activity was difficult to appreciate.

A considerable clearance of radioactivity from the blood pool had occurred 24 hr postinjection (Fig. 1). Homogeneous distribution of radioactivity was observed in the

TABLE 1
Scintigraphic Results

Group		Number	Positive scans	Negative scans
1	1A (cutaneous)	3	2	1
	1B (ocular)	19	18	1
2		37	24*	13*
3		44	0	44

*(See tables 2 and 3 for lesion-site study)

TABLE 3
Detection of Occult Disease

Localizations	True-positives
Skin	6
Lymph nodes	6
Brain	3
Lungs	3
Liver	3
Kidney	1
Total	22

lung, liver and intestinal tract, with hyperfixation occasionally in the gallbladder. The uptake in the eyes was symmetrical, weak and nearly always centered by a clearer zone. Clearance curves for relevant organs are given in the Appendix.

Primary melanomas and metastases were detectable as a clear hyperfixation of the tracer. By 18–24 hr postinjection, tumoral images were considered to be of high quality and their interpretation gave the highest lesion sensitivity for previously known lesions.

The results are summarized in Table 1 according to patient groups and in Table 2 according to the known localizations of Group 2. In Group 2, 22 sites of occult disease were discovered, later correlated with malignant melanoma and correctly accounted for as true positives (Table 3). The Mac Nemar test gave a significant difference at 5% for the patient study (110 patients), and for lesion-site study (104 lesions). When we applied the test organ by organ, we observed no significant difference except for skin and adrenals. The parameters of sensitivity, specificity, diagnostic accuracy, positive and negative predictive values are given in Table 4 on two bases: according to patients entered in the study and according to lesion sites.

For primary cutaneous melanomas (Group 1A), we were not able to visualize a lesion at level I of the Clark classification with a thickness of 1 mm on the Breslow index. This negative result can be explained because of the extremely low thickness. Isotope uptake was related to tumor size which was a limit for detection by the gamma camera. No tumor less than 7 mm in diameter was imaged and this corresponds to the resolution limit of the method. In some cases of multiple cutaneous and subcutaneous nodules, it was difficult to enumerate the lesions detected.

In suspected ocular melanoma, we achieved 18 positive scintigraphies in 19 patients. In 18 cases, we had a clear, intense, homogeneous hyperfixation of the pathological eye (Fig. 2). Maximal differential count between the eyes was up to 60% for a tumor size 15 × 18 × 16 mm and the minimal value was 8% for a tumor size 8 × 6 mm (22 pixels, 64 × 64 matrix).

In Group 1B, the overall sensitivity of BZA scintigraphy was 95%. The relative higher uptake in the melanoma-eye depended on the characteristics of the tumor; size, localization, pigmentation and vascularization. We are presently developing a method to calculate characteristic values which would provide automatic separation between normal and abnormal fixation on both eyes. This method is derived from textural analysis approaches (*11*).

For the patients who underwent enucleation, the lesion was confirmed by histopathology to be a melanoma. Other patients were treated by radiotherapy (either radioactive plaques or protons) and a BZA-scintigraphy showed the absence of ocular hyperfixation 3–6 mo post-treatment. One patient with a choroidal MM (10 × 10 × 5 mm) was a false negative with a symmetrical uptake. This patient had

TABLE 2
Results for Group 2 According to the Known Localizations

Localizations	Number	True positives	False negatives
Skin	21	14	7
Lymph nodes	8	6	2
Bone	9	8	1
Brain	2	1	1
Lungs	4	3	1
Liver	6	6	0
Kidney	2	2	0
Adrenals	4	0	4
Others*	4	2	2
Total	60	42	18

*eye, meningitis, peridural, ascites

TABLE 4
Statistical Parameters

	On a patient basis	On a lesion site basis
Sensitivity	73%	81%
Specificity	100%	100%
Accuracy	85%	87%
Positive predictive value	100%	100%
Negative predictive value	76%	72%

FIGURE 2. Scan showing the head (anterior) 24 hr after injection. Increased uptake is visible on the left eye.

a previous history of radiotherapy for a glioma of the optic chiasma and the lesion was nearly achromic (Fig. 3).

In Group 2, 42 lesions were visualized out of a total of 55 already documented at the time of the study. False negatives corresponded to micro superficial cutaneous lesions (<7 mm), amelanotic melanomas or to anatomical localizations (adrenals). Analysis of individual sites determined to be positive by scanning revealed that kidney, liver, bone, lung, brain and lymph nodes accounted for the highest percentages of metastatic sites imaged with an accuracy of 80%–100% (Table 5).

Figure 4 shows in situ orbital recurrence, multiple liver metastases and diffuse bone infiltration by metastases 6 yr after a primary ocular melanoma was treated by surgery.

Occult disease was detected in 22 sites (Table 3). The melanoma nature of these 22 lesions was confirmed by x-ray, CT, ultrasound, surgery-biopsy and/or the subsequent clinical progress of the disease. The detection of occult metastatic lesions indicates that BZA-scintigraphy

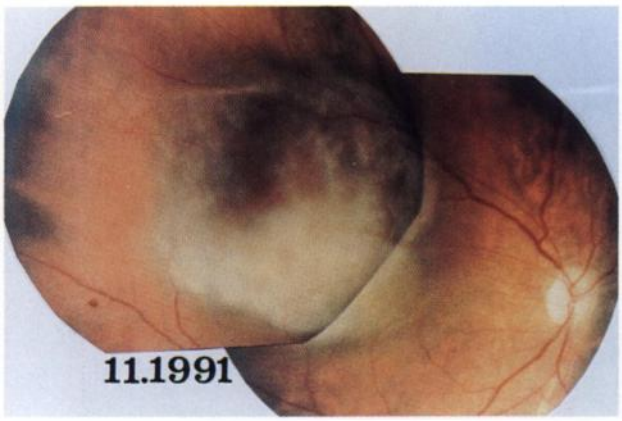

FIGURE 3. Fundus oculi, nearly amelanotic tumor.

TABLE 5
Sensitivity of ^{123}I-BZA for Melanoma Localizations

Localization	Positive scans/ known lesions	Sensitivity
Kidney	3/3	100%
Liver	9/9	100%
Bone	8/9	89%
Lung	6/7	86%
Brain	4/5	80%
Lymph nodes	12/14	80%
Skin	20/27	74%
Adrenal glands	0/4	0%

can provide useful information and have a clinical benefit leading to more appropriate therapy.

Figure 5 shows two hyperfixations of the tracer on an anterior view of the skull. The posterior view (not shown) shows a third hyperfixation. An ophthalmoscopic examination ruled out the diagnosis of ocular melanoma for the increased uptake in projection on the right orbit and CT scans (Figs. 6 and 7) indicate the presence of multiple brain metastases. Figure 8 is an example of lung metastasis.

In Group 3, the 44 scans were normal, as was the check-up by conventional imaging methods. No hyperfixation was noted.

In the patients who underwent the scintigraphy as differential diagnosis, all the scintigraphies were normal. Later, those seven patients were diagnosed with ocular nevus, retinal detachment, biphasic synovial sarcoma of the left thigh, anaplasic adenocarcinoma of the canal duct, thyroid lymphoma, invasive well-differentiated malpighian carcinoma of the esophagus and systemic adenocarcinoma.

Concordance of the results obtained when scintigraphy was repeated on two or more occasions indicates that the

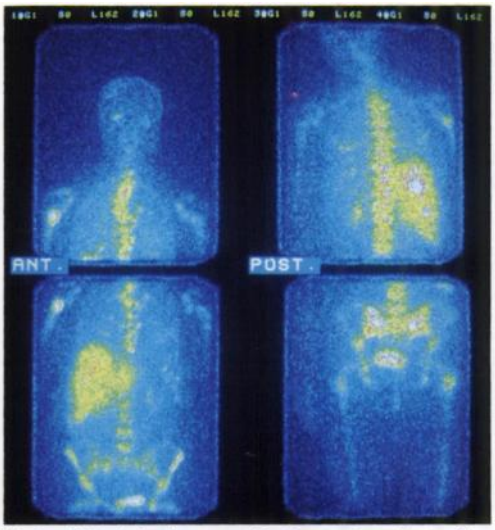

FIGURE 4. Whole-body scan of a Group 2 patient with recurrent melanoma in the orbit, multiple suspected liver metastases and diffuse bone infiltration by metastases.

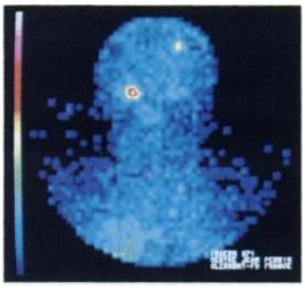

FIGURE 5. Anterior scan of the head taken 22 hr after injection. Two lesions which could be brain metastases are visible.

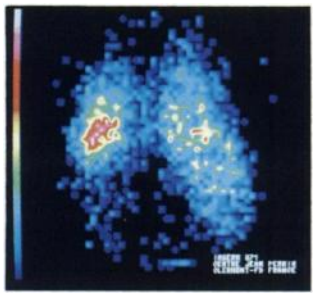

FIGURE 8. Lung metastases. Posterior scan taken 22 hr after intravenous injection of ^{123}I-BZA.

procedure is replicable. We never observed false-positive scans in these studies.

DISCUSSION

The feasibility of the ^{123}I-BZA imaging method is demonstrated with a sensitivity >80% and a specificity and positive predictive value of 100% on a lesion-site basis. These high values for customary parameters are a requisite for a valuable diagnosis in this type of pathology. This diagnostic modality is particularly useful in a territory of difficult diagnosis such as ocular melanoma in which a conservative treatment is now possible for small tumors when detected early. It is also a sensitive and safe method of detecting metastatic melanomas. The present scans imaged 81% of melanoma localizations and were normal in 44 patients in complete clinical remission. Conversely, patients with occult disease, but with BZA-hyperfixation, were later correctly diagnosed with melanoma metastases. From this investigation we are now able to correlate the false negatives with the tumor size, melanin content or anatomical localizations. Nevertheless, the accuracy of 87% of the BZA-scintigraphy is also very helpful in the following indications:

1. Evaluation of the regional invasion of a primary melanoma.
2. Evaluation of metastatic spread in patients with a known locoregional extension.
3. Detection of unsuspected lesions.
4. Differentiation between malignant and benign lesions for ocular tumors.
5. Evaluation of the results of therapeutic procedures.

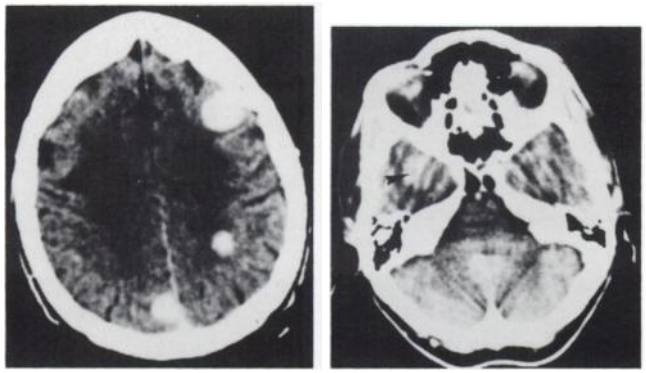

FIGURES 6 and 7. Same patient as in Figure 5. CT scans of different slices indicate the presence of multiple brain metastases. The arrow shows right temporal metastasis.

APPENDIX

Pharmacodynamic Data of BZA

For some patients, anti-coagulated blood was collected from the opposite arm from that in which the injection was made. Whole blood samples were processed for counting. After removal of the whole blood aliquot, the remainder of the sample was centrifuged. Plasma was processed on ultrafree-MC filters (Millipore) in order to obtain bound and free activity. Chromatofocusing of plasma was also performed on a PBE 9-4 column (Pharmacia, 55 × 1 cm) with polybuffer eluant with a pH of 6 at a flow rate of 4 ml/hr. Urine was collected when possible and divided 0–6 hr and 6–24 hr postinjection. Radioactivity of samples was determined. High-performance liquid chromatography (HPLC) analysis of blood and urine samples was performed (*12*).

Blood clearance shows two calculated half-lives: 7.5 min and 4 hr. Plasma clearance closely followed whole blood clearance. Chromatofocusing shows that, at the end of injection, 70% of the BZA was free in the plasma. Five minutes postinjection, 70% of the radioactivity was bound to albumin. One hour postinjection, 80%–85% of the radioactivity was bound to albumin. No interaction with formed blood elements was observed. In the blood, HPLC analysis showed 20%–50% of unchanged compound and 50%–70% of p-iodobenzoic acid 1 hr after injection.

Urinary clearance of ^{123}I-BZA was 60%–85% of the injected dose by 24 hr postinjection (depending in part on the diuresis). In the urine collected between 0 and 6 hr, HPLC analysis shows that the radioactive species were 65%–85% p-iodobenzoic acid and from 6 to 24 hr, 85%–90% p-iodobenzoic acid. At the same postinjection times, about 5% of unchanged compound and 4% of dealkylated derivative (N-2-monoethylaminoethyl 4-iodobenzamide) were detected.

Pharmacokinetic Data of the Tracer

Figure A1 presents the time-activity curves during the first hour postinjection for relevant organs. Table A1 presents an example of quantification: regions of interest

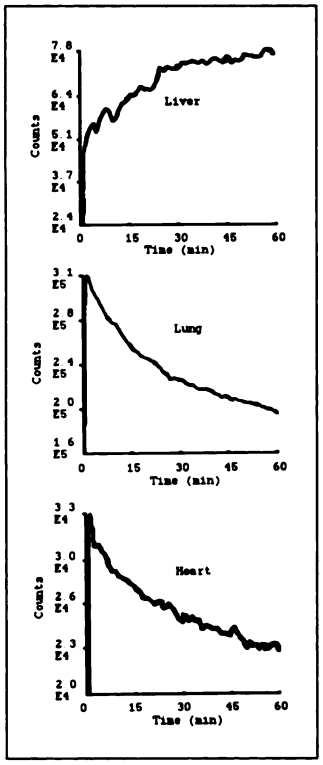

FIGURE A1. Time-activity curves for relevant organs during the first hour postinjection.

(ROIs) were drawn around each organ. The percent of fixation of organs at different times postinjection is expressed according to the injected dose (measured in the syringe). Table A2 shows the percent uptake for relevant organs at delayed imaging times for patients in clinical remission and patients of Group 2 with metastases on these organs.

Organ-to-background ratios at 24 hr postinjection were 1.6 ± 0.17 for the lung (n = 16) and 4.61 ± 0.97 for the liver (n = 10).

Based on preclinical data (*10*), the optimal time for imaging in humans was confirmed to be between 18–24 hr postinjection with the best signal-to-background ratio.

TABLE A2
Percentage Uptake at Postinjection Delayed Times (18 to 24 hr) for Relevant Organs*

	Normal	Metastases
Liver	12%–20%	>30%
Lung	4%–9%	>15%
Skull	3%–6%	>10%

*Patients of Group 3, normal (n = 10) and Group 2, metastases on these organs (n = 5) (injected activity measured in the syringe).

ACKNOWLEDGMENTS

The authors thank Dr. J.Y. Boire for help with the statistical analysis; Mrs. J. Lefrançois for her very professional typing; and R.J. Ferguson for constructive comments on the manuscript. A preliminary report of this data was presented at the European Association of Nuclear Medicine Congress, Vienna, Austria (*Eur J Nucl Med* 1991;18:547). This study was supported in part by a grant from the Fédération Régionale des Centres de Lutte contre le Cancer.

REFERENCES

1. MacKimmie M. W A melanoma toll soars. *The West Australian*, July 10, 1992.
2. Belli F, Sintinami M, Baldini MT, et al. Clinical status of diagnosis and therapy of malignant melanoma. *Nucl Med Biol* 1989;16:621–624.
3. Van Langevelde A, Bakker CNM, Boer H, et al. Potential radiopharmaceuticals for the detection of ocular melanoma. Part II. Iodoquinoline derivatives and ^{67}Ga citrate. *Eur J Nucl Med* 1986;12:96–104.
4. Coderre JA, Packer S, Fairchild RG, et al. Iodothiouracil as a melanoma localizing agent. *J Nucl Med* 1986;27:1157–1164.
5. Hoffer P. Status of Gallium-67 in tumor detection. *J Nucl Med* 1980;21:394–398.
6. Granowska M, Britton KE. Radiolabelled monoclonal antibodies in oncology II. Clinical applications in diagnosis. *Nucl Med Commun* 1991;12:83–98.
7. Siccardi AG, Buraggi GL, Callegaro L, et al. Multicentre study of immunoscintigraphy with radiolabelled monoclonal antibodies in patients with melanoma. *Cancer Res* 1986;46:4817–4822.
8. Bomanji J, Hungerford JL, Granowska M, Britton KE. Radioimmunoscin-

TABLE A1
Percent Uptake Over Time for Relevant Organs of One Patient*

Organ	Time postinjection					
	15 min	80 min	140 min	260 min	330 min	24 hr
Lung anterior	82	51	40	26	18	4
Lung posterior	62	47	38	25	18	4
Liver anterior	87	100	81	54	41	11
Liver posterior	83	100	80	58	42	10
Skull anterior	38	32	25	15	11	3
Background	13	20	22	10	8	6

*Injected activity measured in the syringe.

tigraphy of ocular melanoma with ^{99m}Tc-labelled cutaneous melanoma antibody fragments. *Br J Ophthalmol* 1987;71:651–658.
9. Cis Biointernational-INSERM. Agents for diagnosing and treating melanomas. Aromatic halogenated derivatives usable as such agents and their preparation. *International Patent Num. Pub. WO 90 9170.*
10. Michelot JM, Moreau MF, Labarre PG, et al. Synthesis and evaluation of new iodine-125 radiopharmaceuticals as potential tracers for malignant melanoma. *J Nucl Med* 1991;32:1573–1580.
11. Haralick RM, Schanmugamk, Dinstein I. Textural features for image classification *IEEE Trans Syst, Manual Cybern* 1973;3:610–621.
12. Abstract of XXIX Colloque de médecine nucléaire de langue française. In: *L'Union Médicale du Canada* 1990;07–08:16.

(continued from page 5A)

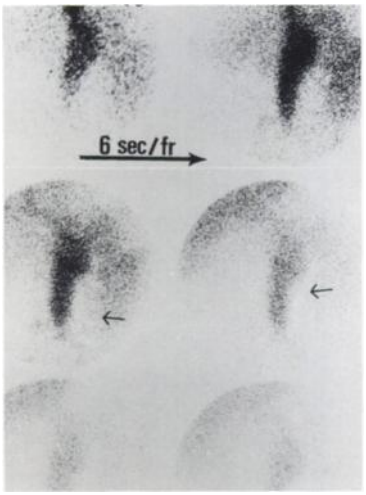

FIGURE 1

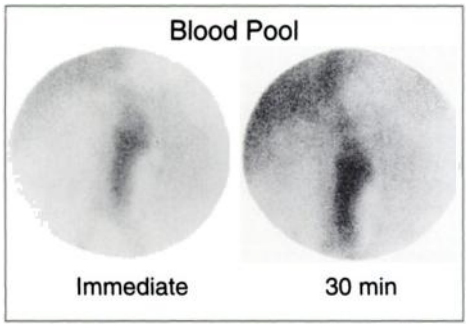

FIGURE 2

FIRST IMPRESSIONS

PURPOSE
A 56-yr-old man with abdominal aortic aneurysm (AAA) was referred for gated cardiac imaging for preoperative evaluation. On anterior first-pass study every second per image immediate and 30-min blood-pool images, a long segment of abdominal aortic aneurysm with a longitudinal cold area (arrow) along the left side of the aortic wall and "angulation" sign were noted. The configuration of the AAA matched the aortogram. The cold area corresponding to the large mural thrombus was located between the functioning calibre of the aneurysm and left abdominal activity outside the abdominal aortic wall. Concurrent abdominal computed tomography and sonography revealed a large abdominal aortic aneurysm with a large thrombus, which was confirmed during surgical repair of the AAA.

TRACER
Technetium-99m-DTPA (28 mCi).

ROUTE OF ADMINISTRATION
Intravenous injection.

TIME AFTER INJECTION
First-pass study, immediate blood-pool study and 30-min blood-pool study.

INSTRUMENTATION
Siemens portal gamma camera with a LEAP collimator.

CONTRIBUTORS
W.J. Shih, A. Kazmers, T. Lawson and V. Stipp.

INSTITUTIONS
Department of Veterans Affairs Medical Center and University of Kentucky Medical Center, Lexington, KY.

FIGURE 3

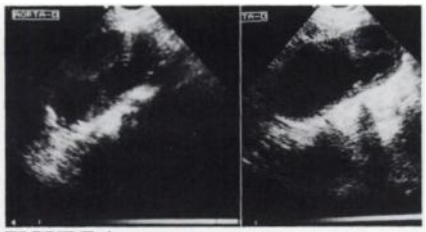

FIGURE 4

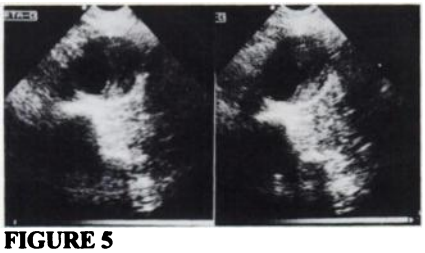

FIGURE 5

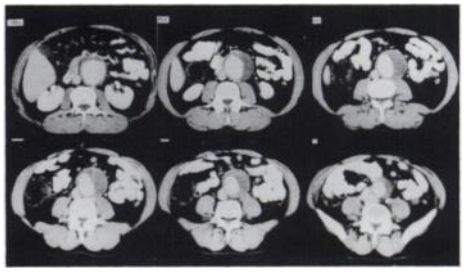

FIGURE 6